

Pressure-based methodologies for zero Mach and low Mach flow simulations

Pascal Bruel

► To cite this version:

Pascal Bruel. Pressure-based methodologies for zero Mach and low Mach flow simulations. Workshop “ Non Linear Phenomena and Dynamics of Flame Propagation ”, Sep 2019, Bourabay, Kazakhstan. hal-02379004

HAL Id: hal-02379004

<https://hal.inria.fr/hal-02379004>

Submitted on 25 Nov 2019

HAL is a multi-disciplinary open access archive for the deposit and dissemination of scientific research documents, whether they are published or not. The documents may come from teaching and research institutions in France or abroad, or from public or private research centers.

L'archive ouverte pluridisciplinaire **HAL**, est destinée au dépôt et à la diffusion de documents scientifiques de niveau recherche, publiés ou non, émanant des établissements d'enseignement et de recherche français ou étrangers, des laboratoires publics ou privés.

Pressure-based methodologies for zero Mach and low Mach flow simulations

Pascal Bruel

Centre National de la Recherche Scientifique (CNRS)

(pascal.bruel@univ-pau.fr)

Laboratoire de Mathématiques et de leurs Applications de Pau (France)

CNRS-Inria-UPPA Cagire team

www.inria.fr/en/teams/cagire

Workshop

« Non Linear Phenomena and Dynamics of Flame Propagation »

Burabay - Kazakhstan

September 2019

Here is my lab !



Pau University (~ 10000 students)

Presentation Layout

1. Mach zero vs low Mach flows.
2. The artificial compressibility method for the simulation of Mach zero reacting flows.
3. The MIAU pressure based approach for the simulation of low Mach flows.

1. Mach zero vs low Mach flows

Compressible Euler equations for a polytropic ideal gas: dimensionless form (Müller, 1999):

$$\frac{t_{conv}}{t_{ref}} \frac{\partial \rho^*}{\partial t^*} + \nabla^* \cdot (\rho^* \mathbf{u}^*) = 0$$

$$\frac{t_{conv}}{t_{ref}} \frac{\partial \rho^* \mathbf{u}^*}{\partial t^*} + \nabla^* \cdot (\rho^* \mathbf{u}^* \otimes \mathbf{u}^*) = -\frac{1}{\hat{M}^2} \nabla^* p^*$$

$$\frac{t_{conv}}{t_{ref}} \frac{\partial \rho^* E^*}{\partial t^*} + \nabla^* \cdot (\rho^* \mathbf{u}^* H^*) = 0$$

with :

$$\rho^* = \rho / \rho_{ref}; p^* = p / p_{ref}; \mathbf{u}^* = \mathbf{u} / u_{ref}; \nabla^* = L_{ref} \nabla$$

$$t^* = t / t_{ref}; t_{conv} = L_{ref} / u_{ref}; E^* = E / (p_{ref} / \rho_{ref}); e^* = e / (p_{ref} / \rho_{ref}); H^* = H / (p_{ref} / \rho_{ref})$$

$$E^* = e^* + \frac{1}{2} \hat{M}^2 \|\mathbf{u}^*\|^2; H^* = E^* + \frac{p^*}{\rho^*}; p^* = \rho^* T^*; T^* = (\gamma - 1) e^*$$

$$\hat{M} = \sqrt{\gamma} \frac{u_{ref}}{\sqrt{\gamma p_{ref} / \rho_{ref}}} = \sqrt{\gamma} M_{ref}$$

Remark: u_{ref} is the reference convective velocity

$$c_{ref} = \sqrt{\gamma p_{ref} / \rho_{ref}} \text{ is the reference speed of sound}$$

The reference Mach number is chosen as the small parameter

From now on, we shall drop the superscript * for denoting the dimensionless variables and it is assumed that the low Mach number asymptotic analysis can be considered as a regular perturbation.

So each independent variables is expanded in terms of a series $\delta^{(i)}(\hat{M})$

where \hat{M} is the small parameter, for instance:

$$p(\mathbf{x}, t; \hat{M}) = \delta^{(0)}(\hat{M})p^{(0)}(x, t) + \delta^{(1)}(\hat{M})p^{(1)}(x, t) + \delta^{(2)}(\hat{M})p^{(2)}(x, t) + \dots$$

$$u(\mathbf{x}, t; \hat{M}) = \delta^{(0)}(\hat{M})u^{(0)}(x, t) + \delta^{(1)}(\hat{M})u^{(1)}(x, t) + \delta^{(2)}(\hat{M})u^{(2)}(x, t) + \dots$$

$$\rho(\mathbf{x}, t; \hat{M}) = \delta^{(0)}(\hat{M})\rho^{(0)}(x, t) + \delta^{(1)}(\hat{M})\rho^{(1)}(x, t) + \delta^{(2)}(\hat{M})\rho^{(2)}(x, t) + \dots$$

the scaling functions are chosen such that:

$$\delta^{(i)}(\hat{M}) = \hat{M}^i$$

Methodology : inject these expansions into the governing equations and order the powers of \hat{M} .

One-scale expansion at low Mach: the hydrodynamic limit

One-scale expansion at low Mach: the hydrodynamic limit

Choose $t_{ref} = (L_{ref} / u_{ref})$

So $t_{ref} = t_{conv}$ is the **convective** time scale, the dimensionless system reads now as:

$$\frac{\partial \rho}{\partial t} + \nabla \cdot (\rho \mathbf{u}) = 0$$

$$\frac{\partial \rho \mathbf{u}}{\partial t} + \nabla \cdot (\rho \mathbf{u} \otimes \mathbf{u}) = -\frac{1}{\hat{M}^2} \nabla p$$

$$\frac{\partial \rho E}{\partial t} + \nabla \cdot (\rho \mathbf{u} H) = 0$$

One-scale expansion at low Mach: the hydrodynamic limit

The system for $O(1)$ variables reads as:

$$\frac{\partial \rho^{(0)}}{\partial t} + \nabla \cdot (\rho^{(0)} \mathbf{u}^{(0)}) = 0$$

$$\frac{\partial \rho^{(0)} \mathbf{u}^{(0)}}{\partial t} + \nabla \cdot (\rho^{(0)} \mathbf{u}^{(0)} \otimes \mathbf{u}^{(0)}) = -\nabla p^{(2)}$$

$$\frac{\gamma}{\gamma - 1} \rho^{(0)} \left[\frac{\partial T^{(0)}}{\partial t} + \mathbf{u}^{(0)} \cdot \nabla T^{(0)} \right] = \frac{dp^{(0)}}{dt}$$

$$\rho^{(0)}(x, t) T^{(0)}(x, t) = p^{(0)}(t)$$

This represents the Mach zero system.

One-scale expansion at low Mach: the hydrodynamic limit

With periodic boundary conditions, the kinetic energy defined by:

$$E_{\text{kin}} = \int_{\mathbb{T}_{\text{advect}}} \frac{1}{2} \varrho^{(0)} \|\mathbf{v}^{(0)}\|^2.$$

remains constant in time

One-scale expansion at low Mach: the acoustic limit

One-scale expansion at low Mach: the acoustic limit

Choose now $t_{ref} = (L_{ref} / (c_{ref} / \sqrt{\gamma}))$

So $t_{ref} = t_{ac}$ is now an **acoustic** time scale, the dimensionless system reads now as:

$$\frac{1}{\hat{M}} \frac{\partial \rho}{\partial t} + \nabla \cdot (\rho \mathbf{u}) = 0$$

$$\frac{1}{\hat{M}} \frac{\partial \rho \mathbf{u}}{\partial t} + \nabla \cdot (\rho \mathbf{u} \otimes \mathbf{u}) = -\frac{1}{\hat{M}^2} \nabla p$$

$$\frac{1}{\hat{M}} \frac{\partial \rho E}{\partial t} + \nabla \cdot (\rho \mathbf{u} H) = 0$$

One-scale expansion at low Mach: the acoustic limit

Then, the continuity equation reads as (keeping only the leading terms):

$$\frac{\partial}{\partial t} \rho^{(1)} + \nabla \cdot (\rho^{(0)} \mathbf{u}^{(0)}) + \hat{M}^{-1} \frac{\partial}{\partial t} \rho^{(0)} = 0$$

to be satisfied for all \hat{M} when $\hat{M} \rightarrow 0$

so:

$$\text{Term } \hat{M}^{-1} \rightarrow \frac{\partial}{\partial t} \rho^{(0)} = 0$$

$$\text{Term } \hat{M}^0 \rightarrow \frac{\partial}{\partial t} \rho^{(1)} + \nabla \cdot (\rho^{(0)} \mathbf{u}^{(0)}) = 0$$

combined with the energy equation it yields after some algebra the **linear acoustic equations**:

$$\left\{ \begin{array}{l} \rho^{(0)} \frac{\partial}{\partial t} \mathbf{u}^{(0)} + \nabla p^{(1)} = 0 \\ \frac{\partial}{\partial t} p^{(1)} + \rho^{(0)} c_0^2 \nabla \cdot \mathbf{u}^{(0)} = 0 \text{ with } c_0^2 = \gamma p^{(0)} / \rho^{(0)} \end{array} \right.$$

One-scale expansion at low Mach: the acoustic limit

With periodic boundary conditions, the acoustic energy defined by:

$$E_{\text{acoust}} = \int_{\mathbb{T}_{\text{acoust}}} \left[\frac{1}{2} \widetilde{\varrho^{(0)}} \|\widetilde{\mathbf{v}^{(0)}}\|^2 + \frac{1}{2} \frac{(p^{(1)})^2}{\widetilde{\varrho^{(0)}} (c^{(0)})^2} \right].$$

remains constant in time. Here, the tilde denotes an averaged value over a region of characteristic length of $1/\widehat{M}$

How to get a flavor of the interaction between acoustics and hydrodynamics at low Mach:  Two-time-scale expansion

Low Mach flows: two-time-scale expansion

Using a single space scale and **two** time scales t / t_{conv} and t / t_{ac} , any field variable, for instance for the pressure, is expanded as:

$$p(\mathbf{x}, t; \hat{M}) = p^{(0)}(x, t, \tau) + \hat{M} p^{(1)}(x, t, \tau) + \hat{M}^2 p^{(2)}(x, t, \tau) + O(\hat{M}^3)$$

with $t/t_{conv} \equiv t$ and $t/t_{ac} \equiv \tau$

The time derivative at constant x and \hat{M} yields (chain rule):

$$\left. \frac{\partial}{\partial t} \right|_{\mathbf{x}, \hat{M}} = \frac{\partial}{\partial t} + \frac{1}{\hat{M}} \frac{\partial}{\partial \tau}$$

Low Mach flows: two-time-scale expansion

The first order energy equation can be expressed as:

$$\frac{\partial p^{(1)}}{\partial \tau} + \gamma p^{(0)} \nabla \cdot (\mathbf{u})^{(0)} = \gamma \frac{1}{\text{Pr Re}} \nabla \cdot (\lambda \nabla T)^{(0)} + (\gamma - 1)(\rho q)^{(0)} - \frac{dp^{(0)}}{dt}$$

Differentiating the above equation with respect to τ and subtracting $\gamma p^{(0)}$ times the divergence of the first order momentum equation yields:

$$\frac{\partial^2 p^{(1)}}{\partial \tau^2} - \nabla \cdot (c^{(0)^2} \nabla p^{(1)})^{(0)} = (\gamma - 1) \frac{\partial (\rho q)^{(0)}}{\partial \tau} \quad \text{with } c^{(0)^2} = \gamma \frac{p^{(0)}(t)}{\rho^{(0)}(\mathbf{x}, t)}$$

This is a wave equation and its source is the change **over acoustic time** of the **leading order of the heat release rate**. See the seminal paper by Klein (1995) for a detailed analysis of the two-space-scale expansion.

2. Simulation of Mach zero reacting flows: the artificial compressibility method.

Artificial compressibility approach

Basic idea: introducing a finite artificial sound speed in the system

Continuity equation  **equation for the pressure**

- Proposed by Chorin (1967) for inert flows
- Unsteady inert flows (Soh *et al.* 1988, McHugh *et al.* 2005)
- Extended to **steady** zero Mach number **reacting** flows by Bruel *et al.* (1996).
- Extended to **unsteady** zero Mach number **reacting** flows by Corvellec *et al.* (1999).
- Combined with **an hybrid-mesh finite volume** formulation by Dourado *et al.* (2004)
- Combined with **discontinuous Galerkin finite element** method by Bassi *et al.* (2006)

It is **well suited** to transform a compressible density based code into a code able to deal with zero Mach inert or reacting flows.

Artificial compressibility approach

Artificial compressibility factor: controls the magnitude of the artificial sound speed that distributes the pressure throughout the computational domain

$$\frac{1}{\beta} \frac{\partial \bar{p}}{\partial \tau} + \frac{\partial \bar{\rho}}{\partial t} + \nabla \cdot (\bar{\rho} \bar{U}) = 0$$

Original equation

Pseudo-time term: is brought to zero between two physical time steps

Physical unsteady term: treated as a source term during the convergence loop in pseudo-time.

Artificial compressibility approach

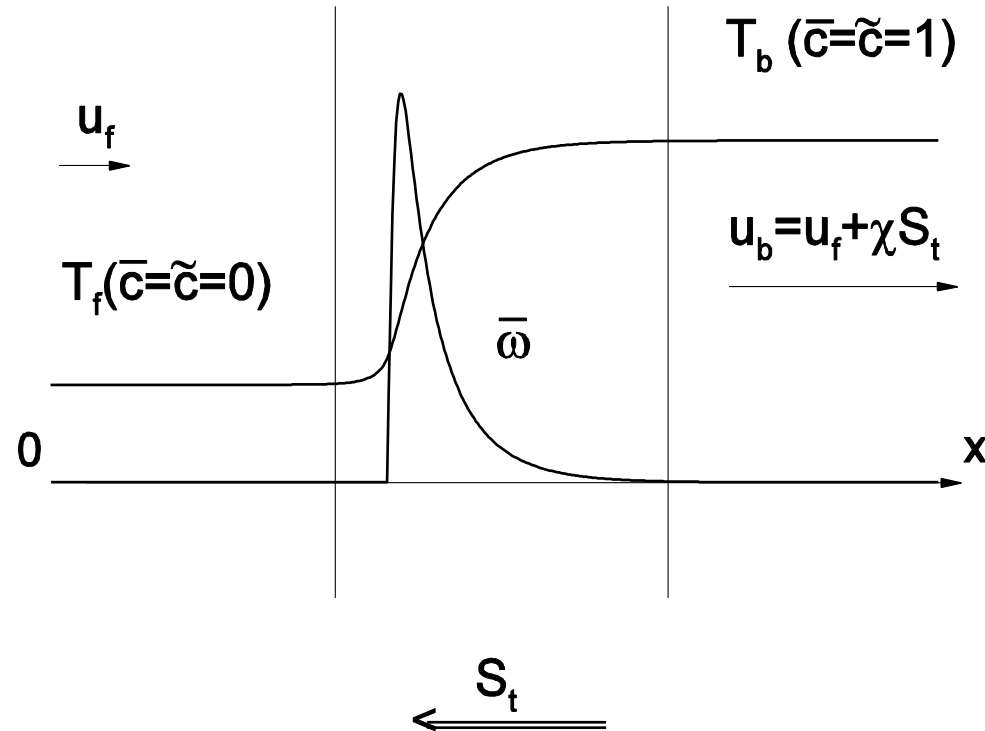
The artificial sound speed is given in constant density flow regions

by $a_c = \sqrt{\tilde{u}^2 + \beta}$

and the corresponding pseudo-Mach number is $M_c = \frac{\tilde{u}}{\sqrt{\tilde{u}^2 + \beta}} < 1$

and its value can be controlled through the setting of β .

Artificial compressibility a concrete example: A simple 1D turbulent premixed flame



With a quenched mean reaction rate, the turbulent flame speed is unique and the flame structure can be determined semi-analytically (Sabel'nikov et al., 1998)

Artificial compressibility a concrete example: A simple 1D turbulent premixed flame

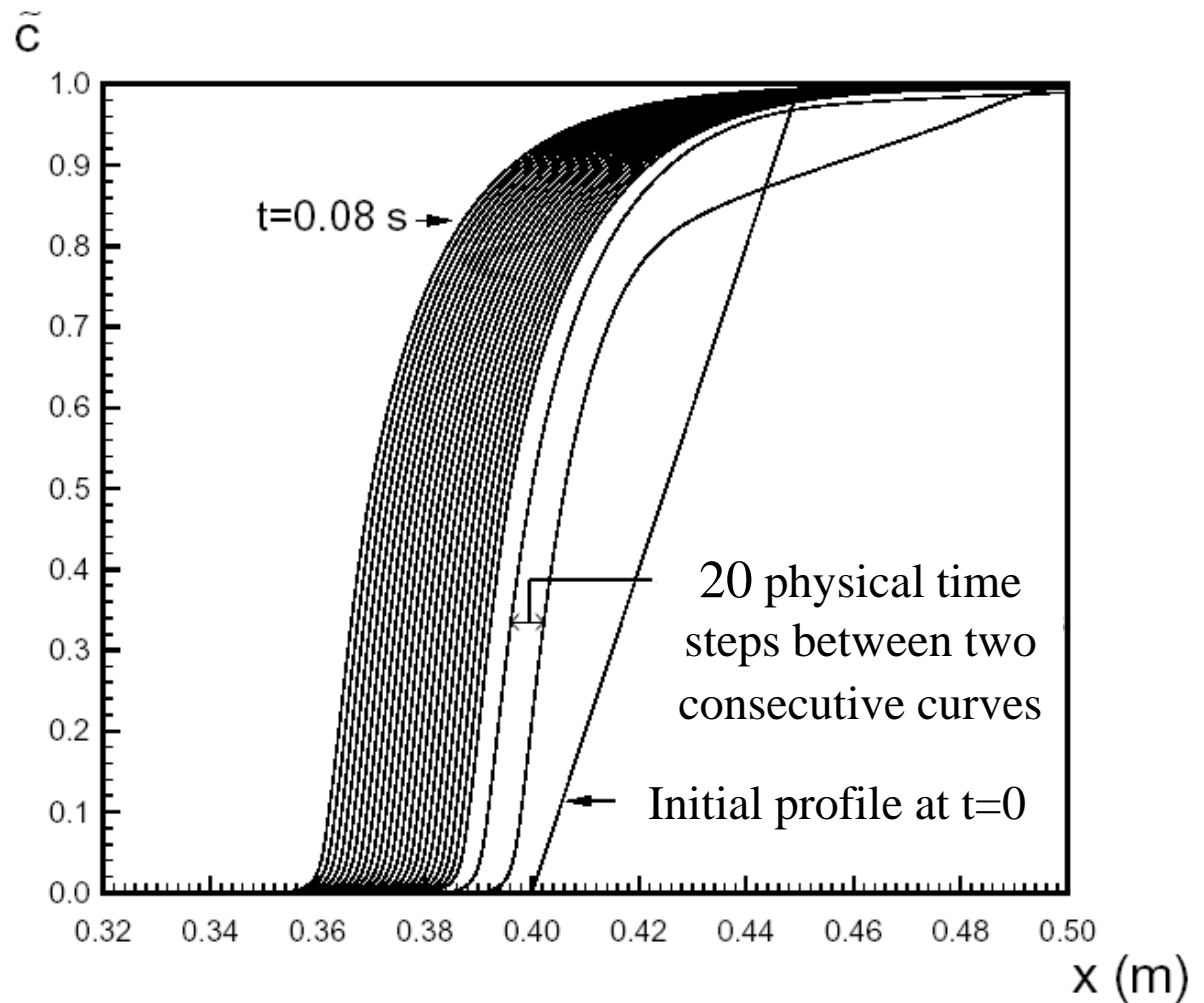
Examples of results, test cases definitions with a continuous quenched mean reaction rate (Corvellec et al., 1999):

	case 1	case 2
χ	5	5
$u_R' (m / s)$	1	10
χc^*	0.03958	0.03958
Λ	0.001	0.001
Sc_t	0.75	0.75
$A_w (kg / m^3 / s)$	1200	48000
$\rho_R (kg / m^3)$	1.1886	1.1886
$\bar{\omega} (kg / m^3 / s)$	$A_w \frac{(\tilde{c} - \chi c^*)(1 - \tilde{c})}{(1 + \chi \tilde{c})^2}$	$A_w \frac{(\tilde{c} - \chi c^*)(1 - \tilde{c})}{(1 + \chi \tilde{c})^2}$

The corresponding theoretical turbulent flame velocity is 0.5 m/s (case 1) and 10 m/s (case 2)

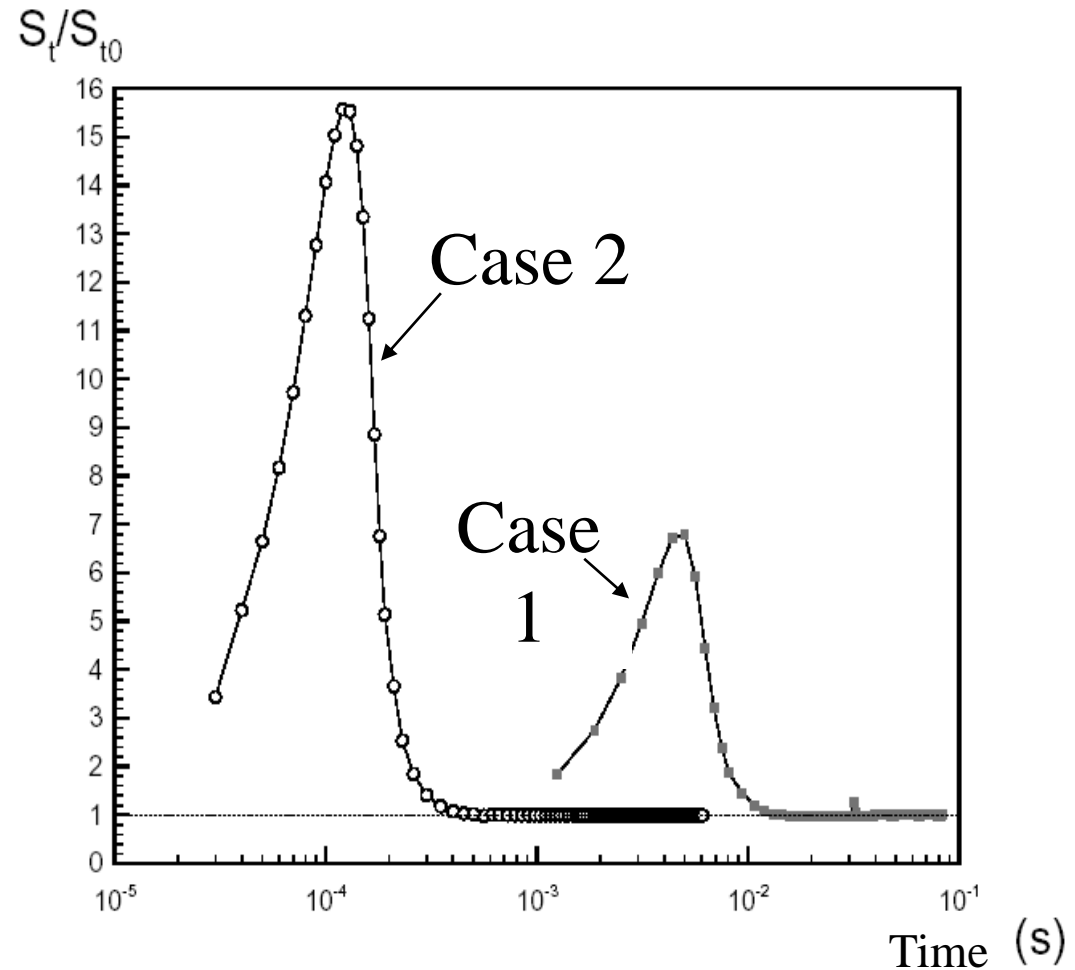
Artificial compressibility a concrete example: A simple 1D turbulent premixed flame

Flame propagation in
case 1



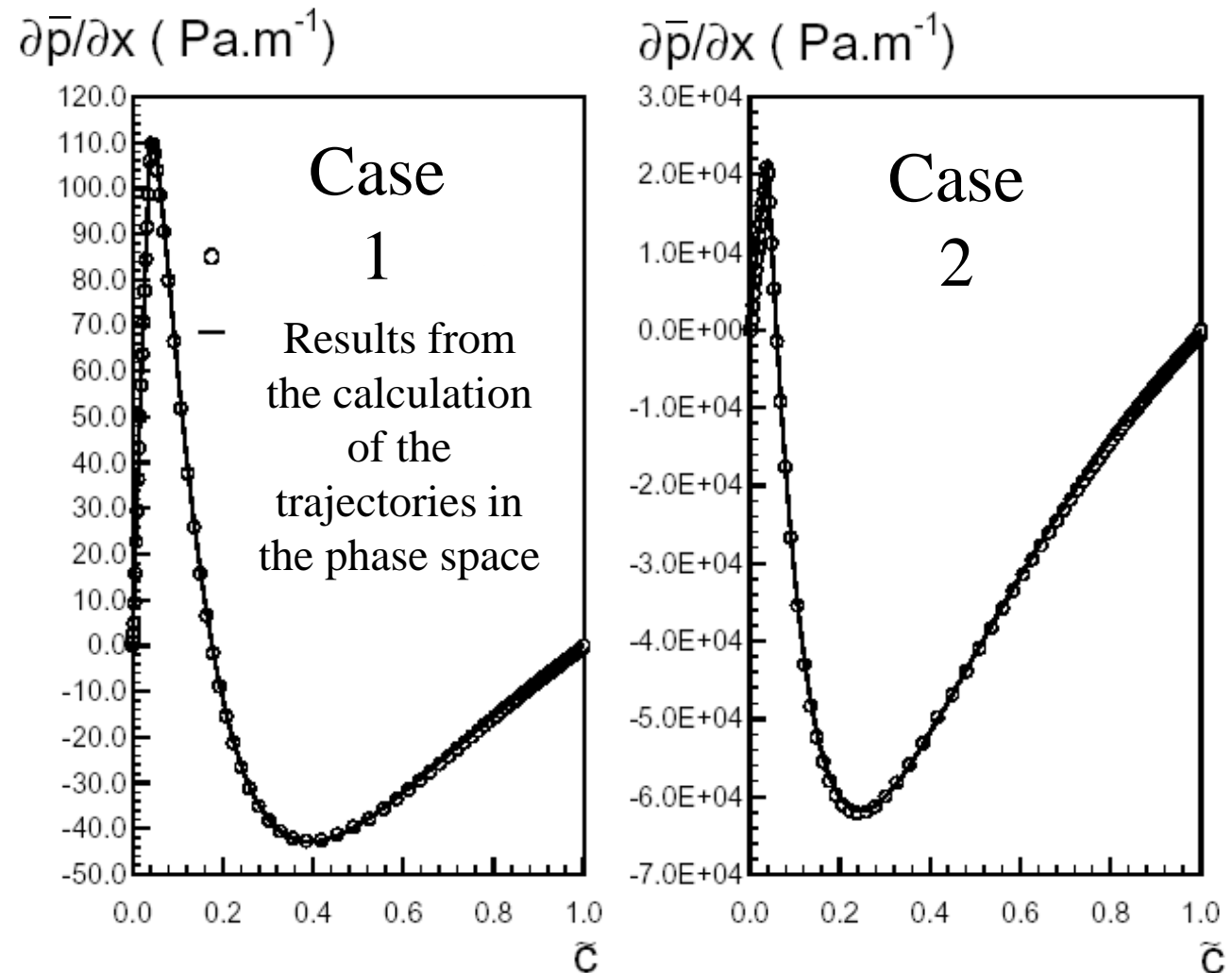
Artificial compressibility a concrete example: A simple 1D turbulent premixed flame

Cases 1 and 2



Artificial compressibility a concrete example: A simple 1D turbulent premixed flame

Pressure
gradient
through the
mean flame
brush



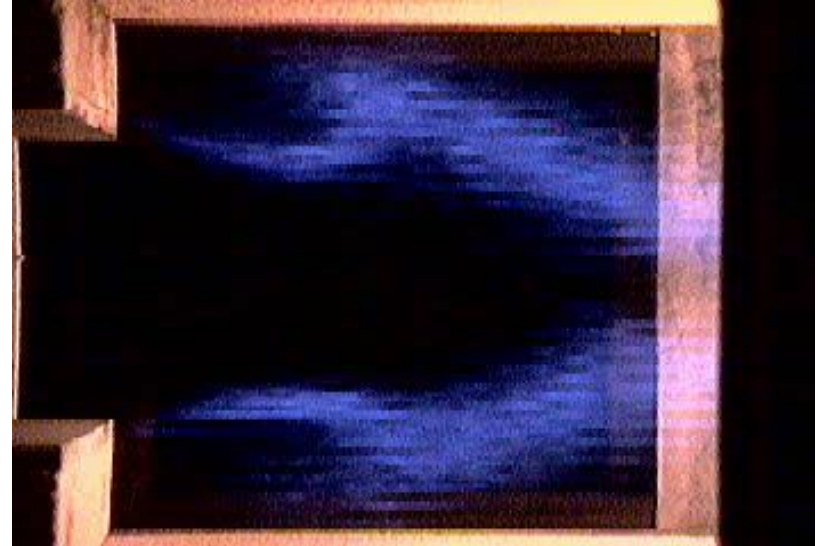
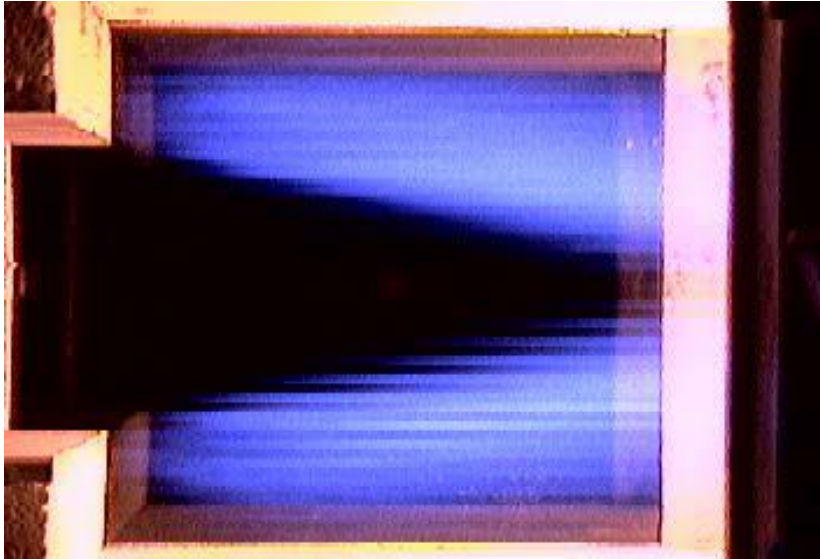
3. Simulation of low Mach flows: the MIAU pressure based approach

Important features of low Mach flows

Any low Mach flow solution results *a priori* from the superimposition/interaction of a slow component (with a quasi-like Mach zero behavior) **and** a fast component (acoustic waves).

The density may vary significantly in relation with the exact nature of the flow at hand (contact discontinuities, reacting flow).

Low Mach flows: illustration of a reacting flows featuring turbulence and coherent motion related with thermoacoustic coupling



Turbulent premixed reaction zone stabilized
by a dump (Nguyen et al., 2009)

Low Mach flows simulations: what are the choices ?

Density-based approach: preconditioning techniques, modification of the diffusion matrix of the flux scheme.

Pressure-based approach: this approach originally developed to cope with Mach zero flows must be adapted: the energy equation plays a key role (Klein, 1995) and so will be used for establishing the pressure correction equation.

The continuous system of PDE's at hand: the Euler equations with a co-located formulation

$$\frac{\partial \rho}{\partial t} + \nabla \cdot (\rho \mathbf{u}) = 0$$

$$\frac{\partial \rho \mathbf{u}}{\partial t} + \nabla \cdot (\rho \mathbf{u} \otimes \mathbf{u}) = -\nabla p$$

$$\frac{\partial \rho E}{\partial t} + \nabla \cdot (\rho \mathbf{u} H) = 0$$

$$E = e + \frac{1}{2} \|\mathbf{u}\|^2 = c_v T + \frac{1}{2} \|\mathbf{u}\|^2 ; H = E + \frac{p}{\rho}$$

$$p = (\gamma - 1) \rho e$$

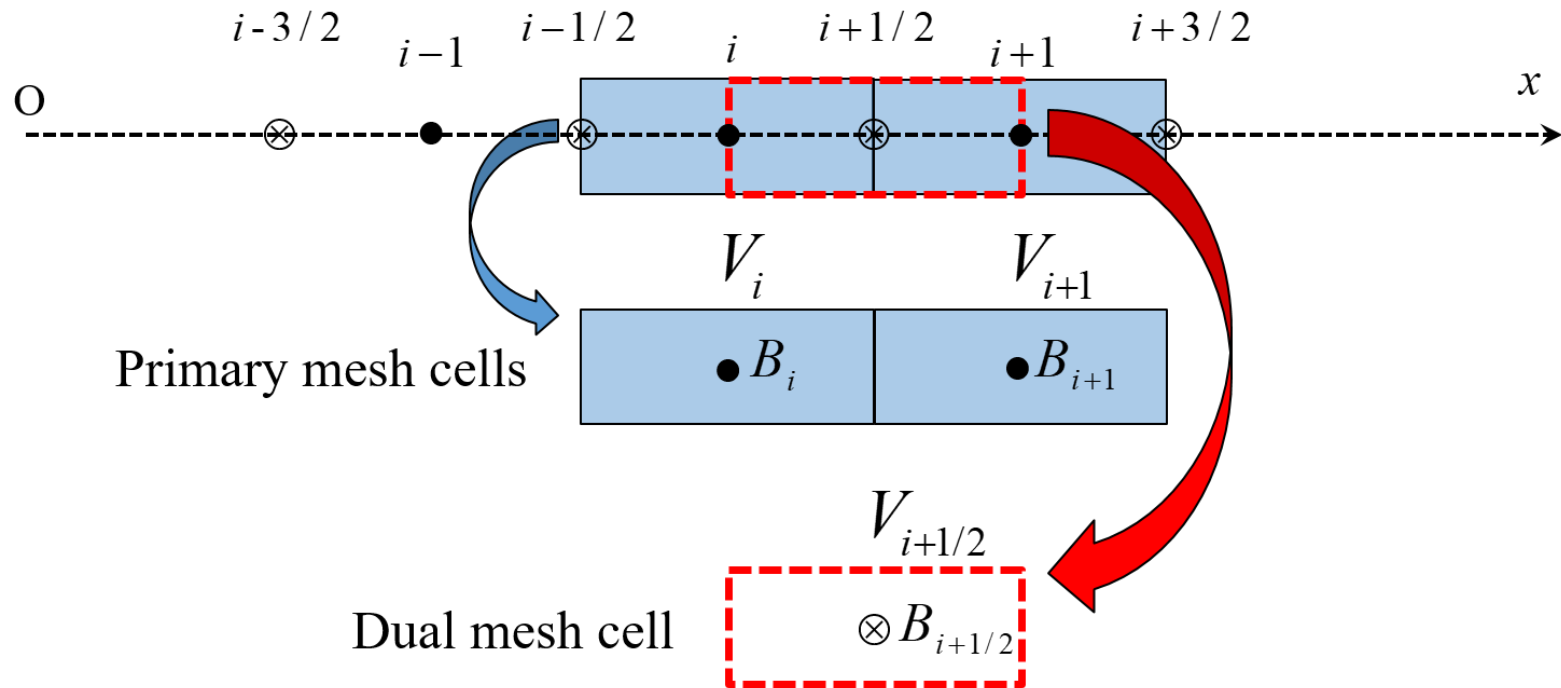
Together with proper initial and boundary conditions

Proposition for a pressure-based algorithm for
simulating non reacting flows
(Moguen et al., 2019)

Predictor step (pressure frozen): solving the continuity and the momentum equations.

Corrector step (density frozen): solving the energy equation to get the pressure correction with input from the momentum equation.

Momentum interpolation method: dual mesh equation



In both steps, the face values on the primal mesh are derived by the MIAU flux scheme to provide the transporting velocity and the face pressure.

The predictor step

- $p_i^* = p_i^k$
- ϱ_i^* from

$$\frac{1}{\Delta t}(\varrho_i^* - \varrho_i^n) + \frac{1}{\Delta x} \left[\varrho_i^* + \frac{1}{2}\psi_i(\varrho^k) \right] v_{i+1/2}^* - \frac{1}{\Delta x} \left[\varrho_{i-1}^* + \frac{1}{2}\psi_{i-1}(\varrho^k) \right] v_{i-1/2}^* = 0$$

- $(\varrho v)_i^*$ from

$$\frac{1}{\Delta t} [(\varrho v)_i^* - (\varrho v)_i^n] + \frac{1}{\Delta x} \left\{ (\varrho v)_i^* + \frac{1}{2}\psi_i [(\varrho v)^k] \right\} v_{i+1/2}^* - \frac{1}{\Delta x} \left\{ (\varrho v)_{i-1}^* + \frac{1}{2}\psi_{i-1} [(\varrho v)^k] \right\} v_{i-1/2}^* + \frac{1}{\Delta x} (p_{i+1/2}^k - p_{i-1/2}^k) = 0$$

- $(\varrho E)_i^* = \frac{p_i^k}{\gamma - 1} + \frac{1}{2} \frac{[(\varrho v)_i^*]^2}{\varrho_i^*}$, $(\varrho H)_i^* = (\varrho E)_i^* + p_i^k$, $h_i^* = \frac{\gamma}{\gamma - 1} \frac{p_i^k}{\varrho_i^*}$

The correction step

- $\varrho^{k+1} = \varrho^*$.
- $p' = p^{k+1} - p^k$ from

$$C_{i-1}p'_{i-1} + C_i p'_i + C_{i+1}p'_{i+1} = -\Sigma_i,$$

where, with the notation $\tau = \Delta t / \Delta x$,

$$C_{i-1} = -\tau \frac{\gamma}{\gamma - 1} v_{i-1/2}^* - \tau \alpha_{i-1/2}^k h_{i-1}^*,$$

$$C_i = \frac{1}{\gamma - 1} + \tau \frac{\gamma}{\gamma - 1} v_{i+1/2}^* + \tau \left(\alpha_{i+1/2}^k h_i^* + \alpha_{i-1/2}^k h_{i-1}^* \right),$$

$$C_{i+1} = -\tau \alpha_{i+1/2}^k h_i^*,$$

$$\begin{aligned} \Sigma_i = & [(\varrho E)_i^* - (\varrho E)_i^n] + \tau \left\{ \frac{1}{2} \frac{[(\varrho v)_i^*]^2}{\varrho_i^*} + \frac{1}{2} \psi_i \left(\frac{1}{2} \frac{[(\varrho v)^k]^2}{\varrho^k} \right) \right\} v_{i+1/2}^* \\ & - \tau \left\{ \frac{1}{2} \frac{[(\varrho v)_{i-1}^*]^2}{\varrho_{i-1}^*} + \frac{1}{2} \psi_{i-1} \left(\frac{1}{2} \frac{[(\varrho v)^k]^2}{\varrho^k} \right) \right\} v_{i-1/2}^* \\ & + \tau \left\{ (\varrho h)_i^* + \frac{1}{2} \psi_i [(\varrho h)^k] \right\} v_{i+1/2}^* - \tau \left\{ (\varrho h)_{i-1}^* + \frac{1}{2} \psi_{i-1} [(\varrho h)^k] \right\} v_{i-1/2}^*. \end{aligned}$$

Updates

$$\varrho_i^{k+1} = \varrho_i^*,$$

$$p_i^{k+1} = p_i^k + p'_i,$$

$$(\varrho v)_i^{k+1} = (\varrho v)_i^* + (\varrho v)'_i = (\varrho v)_i^* - \alpha_i^k (p'_{i+1/2} - p'_{i-1/2}),$$

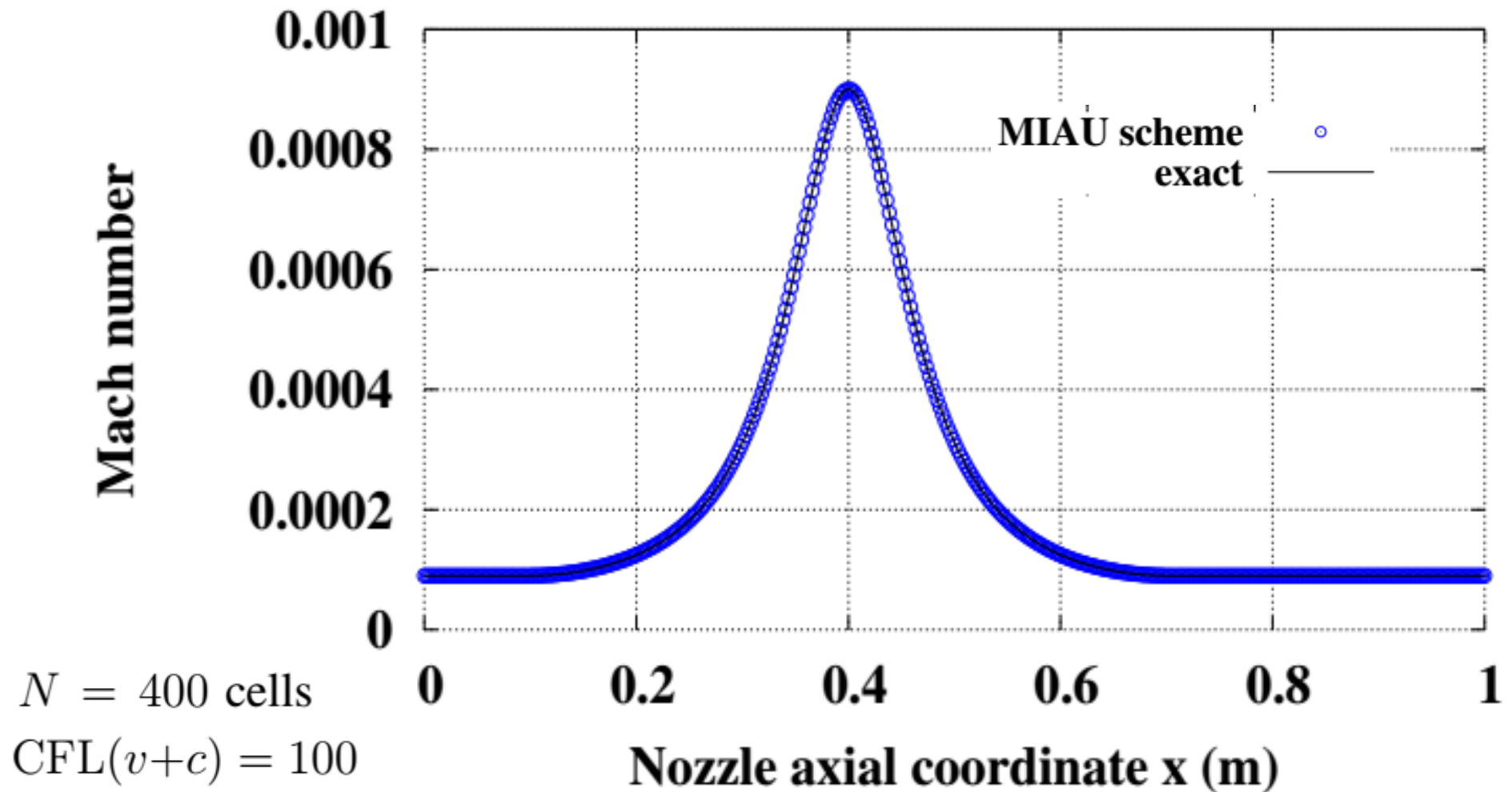
$$(\varrho E)_i^{k+1} = (\varrho E)_i^* + \frac{1}{\gamma - 1} p'_i$$

with

$$p'_{i+1/2} = \frac{1}{2}(p'_i + p'_{i+1}) \quad \text{and} \quad \alpha_i^k = \frac{1}{\frac{\Delta x}{\Delta t} + A_i^k}.$$

A few (~ 5) k-iterations are sufficient to converge the loop.

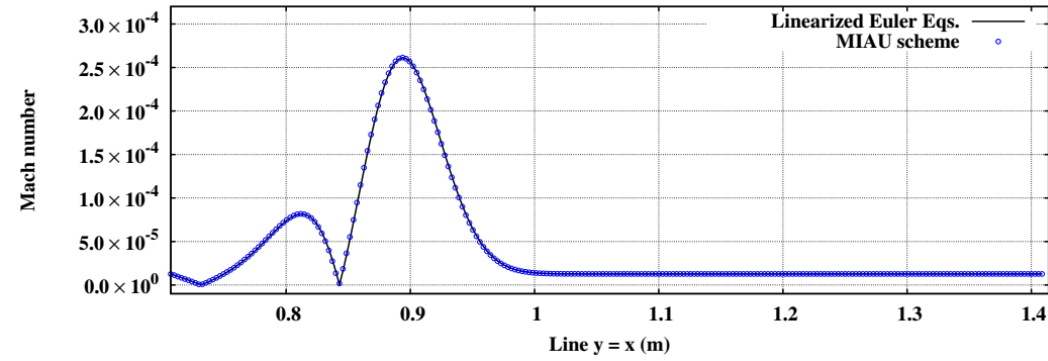
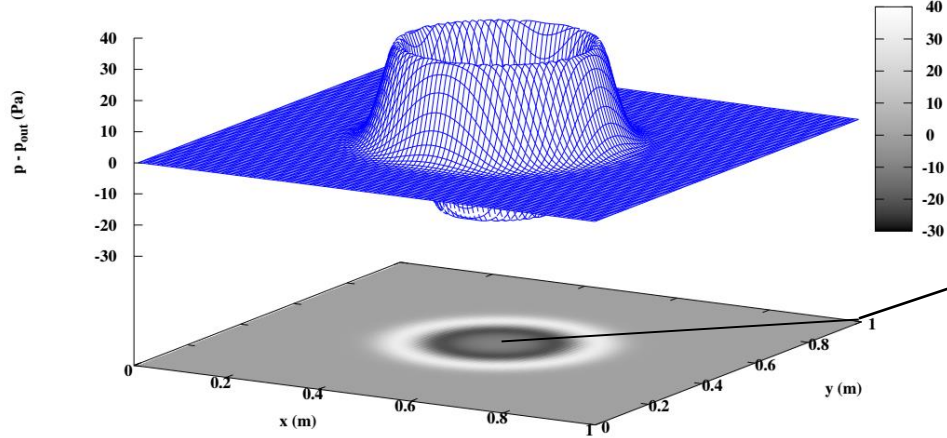
Low Mach flow configuration: nozzle flow



Low Mach flow configuration: acoustic pulse (2D)

$t_f = 0.5$ ms.

Pressure distribution (Pa)



$$(\delta p)^0 = A \exp \left\{ -\alpha \left[(x')^2 + (y')^2 \right] \right\} \text{ (Pa)},$$

$$\text{with } A = 200, \alpha = 1/(0.05)^2, x' = x - 0.5, y' = y - 0.5,$$

$$(\delta \varrho)^0 = (\delta p)^0 / c_0^2 \text{ and } c_0 = \sqrt{\gamma p_0 / \varrho_0}.$$

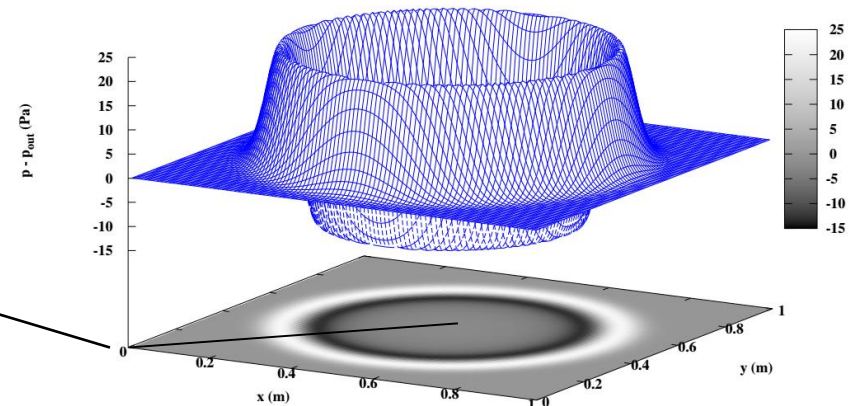
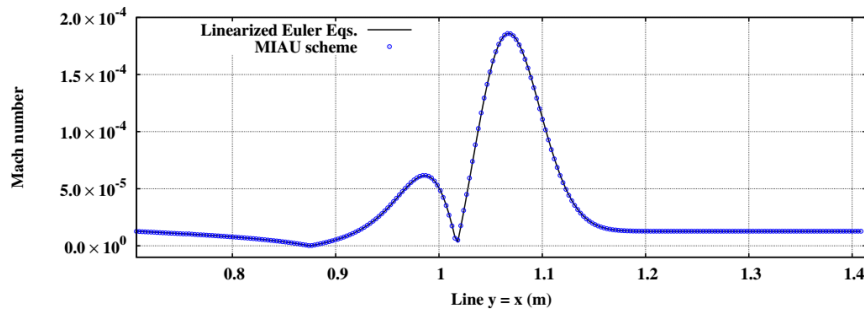
$$\text{CFL}(v_0 + c_0) = 5$$

500 × 500 cells

$$\varrho_0 = 1.2046 \text{ kg/m}^3, u_0 = v_0 = 3.0886 \times 10^{-3} \text{ m/s}, p_0 = 101\,300 \text{ Pa},$$

Pressure distribution (Pa)

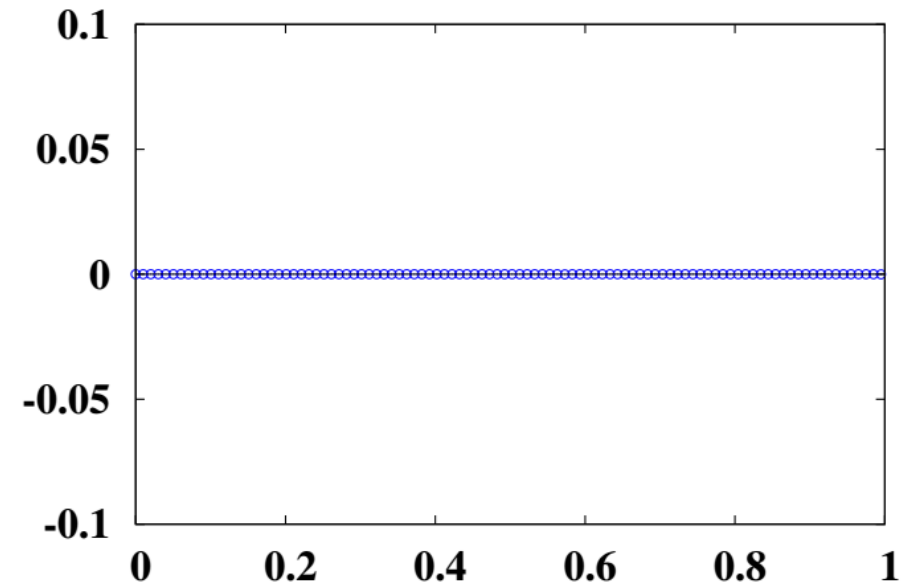
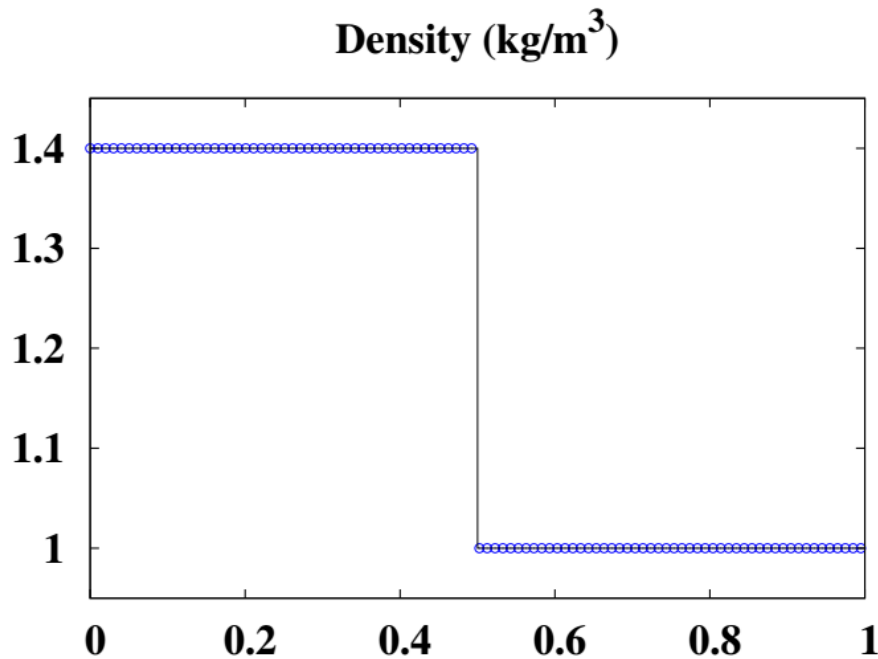
$t_f = 1$ ms.



Low Mach flow configuration: stationary contact discontinuity

ϱ_L (kg/m ³)	v_L (m/s)	p_L (Pa)	ϱ_R (kg/m ³)	v_R (m/s)	p_R (Pa)	t_f (s)
1.4	0	1	1.0	0	1	100

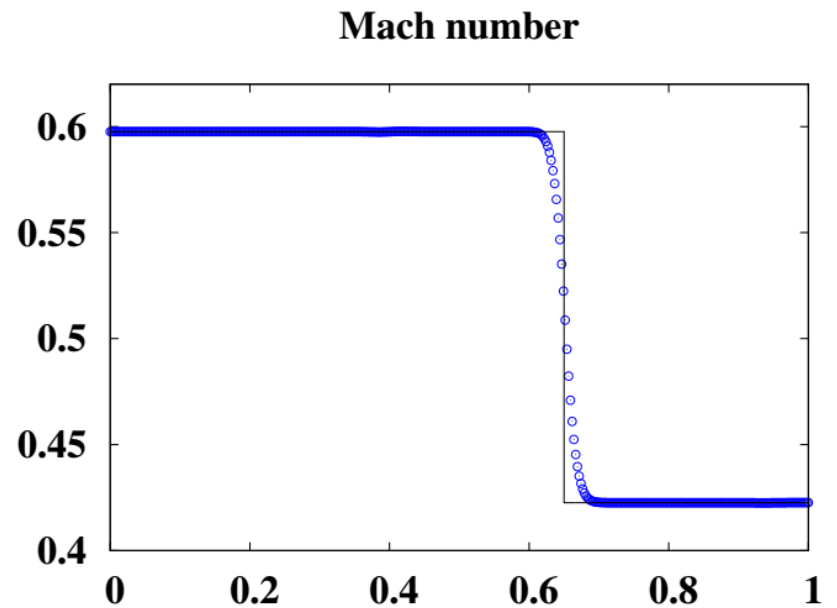
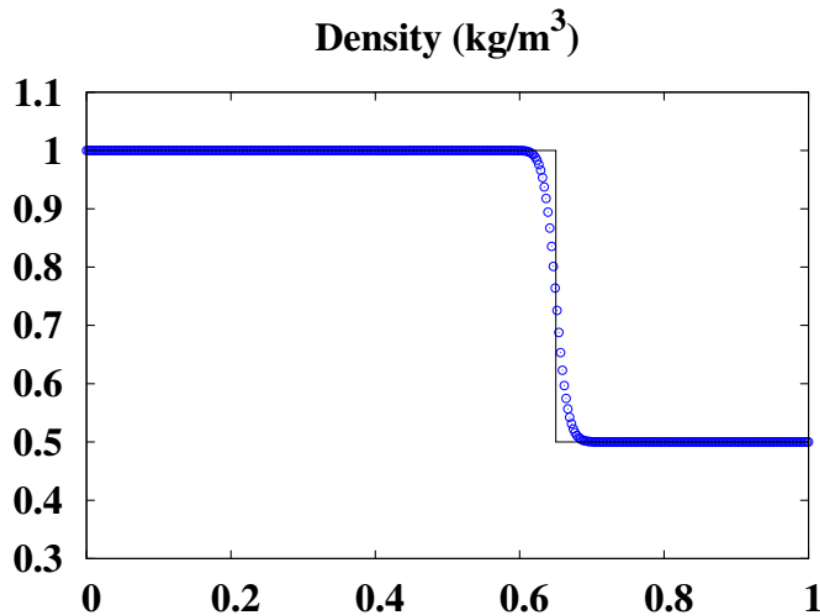
$N = 200$ cells and $\text{CFL}(c_L) = 0.5$



Low Mach flow configuration: moving discontinuity

ϱ_L (kg/m ³)	v_L (m/s)	p_L (Pa)	ϱ_R (kg/m ³)	v_R (m/s)	p_R (Pa)	t_f (s)
1	0.5	0.5	0.5	0.5	0.5	0.3

$N = 400$ cells, CFL = 0.4



Final conclusion

The versatility of pressure based approaches has been demonstrated: able to cope with zero Mach as well as with low Mach flow systems. The MIAU based scheme works also well for high Mach flows (not shown here).

Future work will concentrate on:

Artificial compressibility: increasing the convergence rate by working on the pseudo waves amplitude system at the boundaries.

MIAU like pressure based approach: extending it to reacting flows.

Cited references

- Bassi, F., Massa, F., Botti, L., Colombo, A. (2006) Computers and Fluids, **169**:186-200.
- Bruel, P., Karmed, D., Champion, M. (1996) International Journal of Computational Fluid Dynamics, **7**:291-310.
- Chorin, A. J. (1967) Journal of Computational Physics, **2**:12-26.
- Corvellec, C., Bruel, P., Sabel'nikov, V.A. (1999) International Journal for Numerical Methods in Fluids, **29**:207-227.
- Dourado, M.C.W, Bruel, P., and Azevedo, J.L.F. (2004) International Journal for Numerical Methods in Fluids, **14(10)**:1063-1091.
- Klein, R. (1995) Journal of Computational Physics, **121**:213-237.
- McHugh, P.R. and Ramshaw, J.D. (2005) International Journal for Numerical Methods in Fluids, **21(2)**:141-153.
- Moguen, Y., Bruel, P., and Dick, E. (2019) Journal of Computational Physics, **384**:16-41.
- B. Müller (1999) In 30th Computational Fluid Dynamics Lecture Series, von Karman Institute for Fluid Dynamics, 8-12 March.
- Nguyen, P.D., Bruel, P., and Reichstadt, S. (2009) Flow Turbulence and Combustion, **82**:155-183.
- Soh, W. Y. (1987) Journal of Computational Physics, **70**:232-252.
- Sabel'nikov, V.A., Corvellec, C., Bruel, P. (1998) Combustion and Flame, **113(4)**:492-497.